Composites Science and Technology 182 (2019) 107763

Contents lists available at ScienceDirect

Composites Science and Technology

journal homepage: www.elsevier.com/locate/compscitech

Controlling of resin impregnation and interfacial adhesion in carbon fiber/polycarbonate composites by a spray-coating of polymer on carbon fibers

Ting-Ting Yao[a,b,c], Yu-Ting Liu[a,c], Hong Zhu[a,c], Xiao-Fang Zhang[a,b,c], Gang-Ping Wu[a,b,c,*]

[a] CAS Key Laboratory of Carbon Materials, Institute of Coal Chemistry, Chinese Academy of Sciences, Taiyuan, 030001, China
[b] Center of Materials Science and Optoelectronics Engineering, University of Chinese Academy of Sciences, Beijing, 100049, China
[c] National Engineering Laboratory for Carbon Fiber Technology, Institute of Coal Chemistry, Chinese Academy of Sciences, Taiyuan, 030001, China

ARTICLE INFO

Keywords:
Carbon fiber
Polycarbonate
Impregnation
Interfacial adhesion
Mechanical properties

ABSTRACT

To improve the interfacial properties between carbon fibers (CFs) and polycarbonate (PC) resin, the PC resin was pre-coated onto the CF surfaces by a spray-coating method, and a post-heating process was applied for ensuring uniformity of the coating layer. To further investigate the interfacial interactions between the CFs and the coating layers, the physically-adsorbed PC resins were removed from some coated CFs by washing with solvent. The results showed that the CF/PC interfacial adhesion properties could be related to the coating thickness (or the resin impregnation) and fiber-matrix interactions. For a PC coating layer thinner than 0.15 μm, the PC could not be fully-impregnated into the CF bundles, thus leading to inferior CF/PC interfacial properties and mechanical properties in the final composites; while for a coating layer with thickness ranging from 0.15 to 0.32 μm, it allowed formation of well-impregnated interfaces; if coupled with a further hot-pressing for strengthening the interfacial bonding interactions, both the CF/PC interfacial shear strength and mechanical properties for the corresponding composites were significantly enhanced. The interfacial interactions and reinforcing mechanisms for the CF/PC composites were schematically proposed.

1. Introduction

Carbon fiber reinforced thermoplastics (CFRTPs) are expected to be used as structural parts of aircrafts, automobiles, electrical product shells and sport equipments due to their mechanical properties, such as high specific strength, high specific stiffness, short processing time and high recyclability [1,2]. The properties of a CFRTP composite depend on behaviors of its constituent parts as well as those of interfaces between the fibers and their surrounding resin. Currently, it is generally accepted that mechanical properties, shear resistance, and life expectancy of such composites are largely limited by the bonding strength and stability of their interfaces [3].

To achieve a strong and stable interfacial adhesion for a CFRTP, some conventional methods have been developed to modify the surfaces of CFs, such as oxidation using concentrated nitric acid, electrochemical oxidation [4,5], coating by sizing agents [6,7], plasma treatment, chemical grafting [8,9], and growth of carbon nanotubes or graphene-based materials on CFs [10,11]. Iroh [12] et al. have coated thermoplastic copolyimide onto CF surfaces by electrochemical deposition and the mechanical properties of the corresponding CF/polyimide composite were improved by 25%. Montes-Morán [13] et al. have found that the CF/PC interfacial adhesion could be improved by 15.42% by using a plasma treatment. Yamamoto [14] et al. have improved CF/PMMA interfacial interactions by pre-adsorbing PMMA particles onto the CF surfaces using an electrophoresis process and the interfacial shear strength have been improved by 68%. In general, these CF surface modifications are considered to be able to enhance mechanical anchoring, chemical interaction, physical adsorption or impregnation ability between the CFs and thermoplastic matrix resin, but only to a limited extent [15].

One of the challenging obstacles for improving the CFRTP interfacial properties should be high viscosity of a thermoplastic resin, even in a high temperature, which makes the resin infusion difficult, resulting in poor impregnation of the resin into CFs during a composite-making process. It is well accepted that the inefficient impregnation of a matrix resin will impart poor interfacial adhesion of a CFRTP [16,17], and thus degrade mechanical properties of the composite. Therefore, various impregnation methods have been developed, such as powder impregnation [18], solvent impregnation [19] as well as melt impregnation [20,21]; however, they are still not facile or effective enough to tailor the impregnation and adhesion behaviors of a thermoplastic resin at a CFRTP interface.

* Corresponding author. CAS Key Laboratory of Carbon Materials, Institute of Coal Chemistry, Chinese Academy of Sciences, Taiyuan, 030001, China.
E-mail address: wgp@sxicc.ac.cn (G.-P. Wu).

https://doi.org/10.1016/j.compscitech.2019.107763
Received 30 March 2019; Received in revised form 24 July 2019; Accepted 27 July 2019
Available online 01 August 2019

In this work, the CFs were spray-coated with a thermoplastic resin to achieve a good impregnation of PC into CF bundles, and a post-thermal treatment was performed for ensuring a uniform coating on the CFs. This method has the advantages of good resin impregnation, facile and minimization of solvent use. The results revealed that the CF/PC interfacial adhesion strength could be improved up to 87.8% by the most as compared to that of the un-coated CF/PC, and the interfacial properties were closely correlated to the CF surface chemistry, coating thickness and fiber morphologies, and the mechanical properties of the final composites were also significantly enhanced.

2. Experiments

2.1. Materials

The CFs with sizing agents were supplied by Toho Inc. Corp. (Japan, 12 K) and the PC sheets with thickness of around 0.3 mm and PC powder with particle size of 50–100 μm were supplied by Dongguang Plastic Film Corporation, China. Melt mass flow rate of the PC sheet and PC powder were 1.451 and 1.493 g/min, respectively, indicating similar processing flowability. The measurement method was shown in the supporting information.

2.2. Spray coating of PC on CFs

The as-received CFs were first desized by an acetone-extraction process at reflux for 24 h (denoted as CF_{de}). Some of the desized CFs were further oxidized at 500 °C for 10 min in air, and the oxidized CFs were labeled as CF_{ox}.

The spraying solution was prepared by dissolved a certain amount of PC powders in dichloroethane under ultrasonic assist for 45 min to form a clear solution at ambient temperature. The as-prepared PC solutions were then stored in a sealed glass flask to prevent solvent from volatilizing. By controlling the added amount of PC powders, the spraying solutions with concentrations of 2.5, 5, and 7.5 wt% were obtained; correspondingly, viscosities of the obtained PC solutions were 5.59, 6.57, and 8.16 mPa s respectively, measured by NDJ-8S Digital Rotational Viscometer at room temperature. The #0 rotor was used at a rotating speed of 30 r/min.

The schematic for the fiber coating and post-treatment processes is shown in Fig. 1. For the fiber coating process, the fiber (CF_{de} or CF_{ox}) tows were firstly air-spread by a well-controlled wind, and fixed onto a metal frame; thereafter, the tows were spray-coated with PC solutions by using a spray jet, controlling the spraying amount of about 2.5 ml in 15 s. All the experimental conditions were identical except for the PC concentrations. The coating procedure was conducted on each CF specimen for 45 s. For the post-treatment process, the coated CFs were firstly dried at ambient temperature overnight to remove the solvent. Furthermore, to uniformize the PC coatings on the CFs, all the coated CFs were heat-treated in a tube furnace at 300 °C for 30 min; the as-obtained CFs were denoted as CF-Uni. Table 1 shows abbreviations used for the investigated CFs.

Table 1
Abbreviations used for various samples prepared.

Sample code	Details
CF_{ox}-C	PC solution-coated CF_{ox} without thermal uniformization
CF_{ox}-Uni-0.06	2.5 wt% PC solution-coated CF_{ox} with thickness of 0.06 μm
CF_{ox}-Uni-0.15	5 wt% PC solution-coated CF_{ox} with thickness of 0.15 μm
CF_{ox}-Uni-0.32	7.5 wt% PC solution-coated CF_{ox} with thickness of 0.32 μm
CF_{de}-Uni	5 wt% PC solution-coated CF_{de} with thermal uniformization
CF_{ox}-Uni-w1	CF_{ox}-Uni after washed by solvent
CF_{ox}-Uni-w2	Unidirectional CF_{ox}-Uni/PC after washed by solvent

2.3. Contact angle measurements for the CFs

Contact angle measurements were performed to characterize the "wettability" of the CF surfaces by a molten PC resin. A single CF was straightened and fixed on both sides, and then a small amount of PC powders (diameter of ranging from 25 to 40 μm) were blowed up onto the CF surface. Thereafter, the CF was subjected to a heat-treatment process at 300 °C for 10 min to melt the PC powders for forming molten droplets on the CF. After cooling, the droplets with diameter ranging from 50 to 62.5 μm was selected and their contact angles towards the CF were measured.

2.4. Structural characterizations on the CFs

The morphologies of the CFs were characterized by a field-emission scanning electron microscope (FE-SEM, JEOL, JSM-7001 F, Japan) at an accelerating voltage of 10 kV. The CF surface chemistries were determined by an X-ray photoelectron spectroscopy (XPS). The spectra were obtained using an ESCALAB 250Xi type X-ray photoelectron spectrometer (ThermoFisher, America) with Al Kα (1486.6 eV) X-ray source operated at 75 W.

The Fourier transform infrared spectroscopy-attenuated total reflectance (FTIR-ATR) was used to determine the chemical compositions on the CF surfaces, using a Perkin Elmer Spectrum 100 at a resolution of 0.4 cm^{-1}.

2.5. Tensile strength of the CFs

The tensile strengths of the CFs were determined by using a single fiber stretching machine at 20 mm intervals in its longitudinal direction. The pretension for the single CF was set as 0.01 N, and the stretching rate was 2 mm/min. At least 30 effective tensile strength results were recorded in this study. The statistical distribution of the CF strength data is usually expressed by a two-parameter Weibull equation (given as Eq. (1)) [22,23].

$$F(\sigma) = 1 - exp\left(-L\left(\frac{\sigma}{\sigma_0}\right)^m\right) \quad (1)$$

where σ is the fiber tensile strength, F(σ) the cumulative probability distribution function of the fracture strength, m the Weibull modulus, σ_0

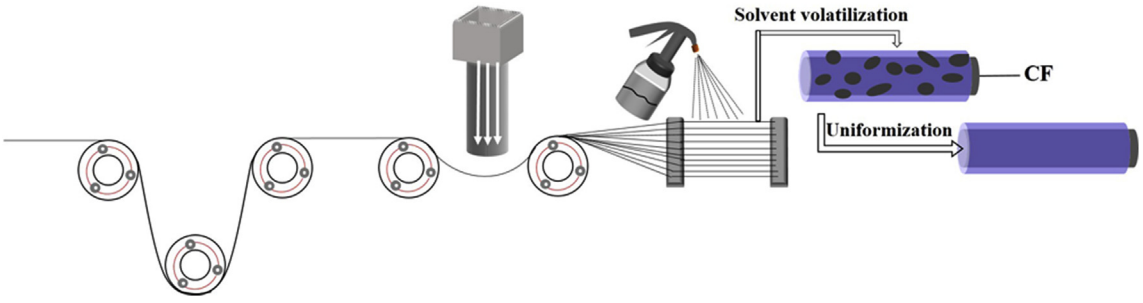

Fig. 1. Schematic for CF spray-coating and thermal uniformization.

the location parameter. The CF tensile strength data plotted in Eq. (2) were linearly fitted, and the parameters σ_0 and m were estimated using the least squares regression method [22].

$$In\left(In\left(\frac{1}{1-F(\sigma)}\right)\right) = mIn(\sigma) - mIn(\sigma_0) + In(L) \quad (2)$$

2.6. Single-filament fragmentation tests

A single fiber was fixed onto a metal frame to complete the spary-coating process under otherwise identical conditions to the CF tows. Then the single CF was sandwiched into two PC sheets and set into a metal mould for hot-pressing. The hot-pressing was conducted at 220 °C for 15 min, and pressured at 4 MPa for 3 min. A dogbone-shaped test specimen with a single CF centered was obtained using a die-punch. The axial line of the embedded CF was parallel to the axial direction in the tensile test. At least ten specimens were fabricated for the fragmentation tests. Then the specimens were tensile-stretched to 7.5% by a mini-tensile machine (Jinan Shidai Shijin Testing Machine Group Co. Ltd, WDW-T2, China) with a crosshead speed of 0.1 mm/min and gauge length of 30 mm. The interfacial shear strength (IFSS) was calculated by the Kelly-Tyson equation [24].

$$\tau = \sigma(l_c)d/2l_c \quad (3)$$

The fiber strength at the critical fragment length (l_c) was calculated using the Weibull weakest-linking theory [25]:

$$l_c = 4/3l_n \quad (4)$$

$$\sigma(l_c) = \sigma(l_o)(l_o/l_c)^{1/m} \quad (5)$$

where τ is the interfacial shear strength, $\sigma(l_c)$ strength of the fiber of the critical length, d the fiber diameter, $\sigma(l_o)$ strength of the fiber with a gauge length of l_o (20 mm).

2.7. Mechanical tests for the composites

To fabricate a composite for the mechanical test, a bundle of CFs was firstly sandwiched between two PC sheets and moulded for hot-pressing. The hot-pressing was conducted at 220 °C for 17 min and pressured at 2.5 MPa during the overall process under vacuum. The CF volume fraction (V_f) of the composites was determined according to the following relationship,

$$V_f = \frac{V_c}{V_c + V_r} = \frac{\rho_r \times M_f}{(\rho_r - \rho_c) \times M_f + \rho_c} \quad (6)$$

where V_c, V_r are the volumes of the CFs and resin matrix in the composite, respectively; ρ_c, ρ_r the densities of the CFs and resin matrix in the composite, respectively; M_f, the weight fraction of the CFs in the composite. The density of the CFs is determined to be 1.76 g/cm^3 and that of PC resin is 1.17 g/cm^3. The M_f of the composites was determined by a difference in sample weight before and after burning in nitrogen. The burning conditions were pre-determined by a thermogravimetric analysis. For the CF_{ox}-Uni/PC composite, as shown in Fig. S1, the sample weight remained almost unchanged up to about 470 °C and the maximal weight loss occurred at about 510 °C. At 600 °C, no obvious weight loss was observed, indicating the completion of the resin decomposition process. Therefore, the burning conditions for the composites were determined to be 600 °C for 30min under nitrogen atmosphere. The composites were then weighted before and after burning to obtain the weight fraction of the CFs in the composites, and the results were shown in Table S1 in the supporting information. The V_f in the CF_{ox}-uni-0.06/PC, CF_{ox}-uni-0.15/PC, CF_{ox}-uni-0.32/PC composites was calculated to be 7.31%, 6.96% and 6.74% respectively. Therefore, these specimens had approximately the same fiber volume fraction.

Tensile tests for the composites were conducted on a universal material testing machine (Jinan Shidai Shijin Testing Machine Group Co. Ltd, WDW-20E, China) in accordance to China National Standard GB/T 3354–1999. The tensile sample dimension was 80 × 10 × 1.5 mm and the crosshead speed was 2 mm/min. The flexural test was carried out according to China National Standard GB/T 1466–2005. The flexural sample dimension was 12 × 2.5 mm with a support span 30 mm in length. The cross-head speed was 2 mm/min. A 90° tensile strength test process (stretching at a direction perpendicular to the CF axis) for the laminate was shown in Fig. 2. At least ten data were recorded and averaged for each specimen.

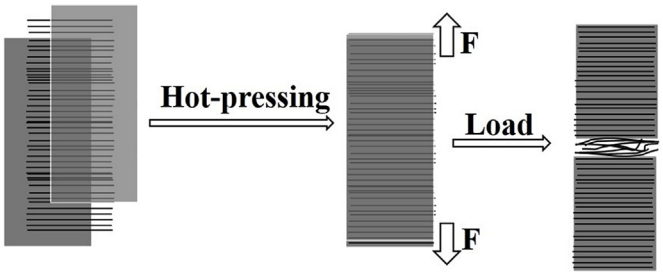

Fig. 2. Schematic for the 90° tensile strength test of a composite laminate.

3. Results and discussion

3.1. Changes in CF surface morphologies

Fig. 3 shows surface morphologies of the CF_{de} and CF_{ox}. Grooves along the fiber axis could hardly be distinguished from the CF_{de} surface (Fig. 3a); contrastively, the grooves on the surfaces of CF_{ox} became clearer, meaning that the CF surface roughness was increased through the air oxidation treatment. From the insets shown in Fig. 3a and b, the contact angle for PC melt droplet on the CF_{ox} was obviously smaller than that on the CF_{de}, suggesting the PC resin had an improved wettability on the CF_{ox} surface. Thus, if not specially noted, the following coating work was performed on the CF_{ox}.

Upon the PC solution immersion and solvent evaporation, the PC-coated CFs presented fully-impregnated but non-uniform morphologies of the PC resin, along with some tubular voids and irregular nubbly particles formed by solvent volatilization (Fig. 3c). In order to obtain CFs with uniform coating, a thermal uniformization process was employed. After the uniformization, the PC coatings became significantly uniform (Fig. 3d). The voids and nubbly particles were mostly disappeared, and thin PC coating layers were formed throughout the CF surfaces (Fig. 3d, e, f), resulting from the good thermal-ductility of PC resin at high temperatures.

In our study, the coating amount of PC on the CF tows could be controlled by viscosity of the PC solution, thus by the PC concentration (Fig. 3g, h, i). We found the ideal PC concentration for the spray-coating was 5–7.5 wt%. Over-high concentration (> 7.5 wt%) would have trouble to make the PC solution spray-out from the sprayer for finishing the coating. The PC concentration in the solution was found to be correlated almost linearly to the coating thickness on the CFs, e.g., the PC thickness was 0.06 μm for 2.5 wt% of PC solution, 0.15 μm for 5 wt %, and 0.32 μm for 7.5 wt%, respectively, corresponding to diameters of 7.11, 7.20 and 7.37 μm, respectively. In our study, the grooves originally found in CF_{ox} were disappeared after the PC coating and the thermal uniformization, indicating that the CF surfaces were smoothed up.

An alternative method for coating a thermoplastic resin on CFs is overlap coating, *i.e.*, subjecting overlapped resin sheets to high temperature and pressure to impregnate into the sandwiched CFs. EL-Dessouky et al. [26] used thermoplastic film of polyphenylene sulphide (PPS) to impregnate the carbon fiber spread-tow (CFST) fabric to obtain laminate by a hot pressing, with a pressure of 60 MPa and temperature

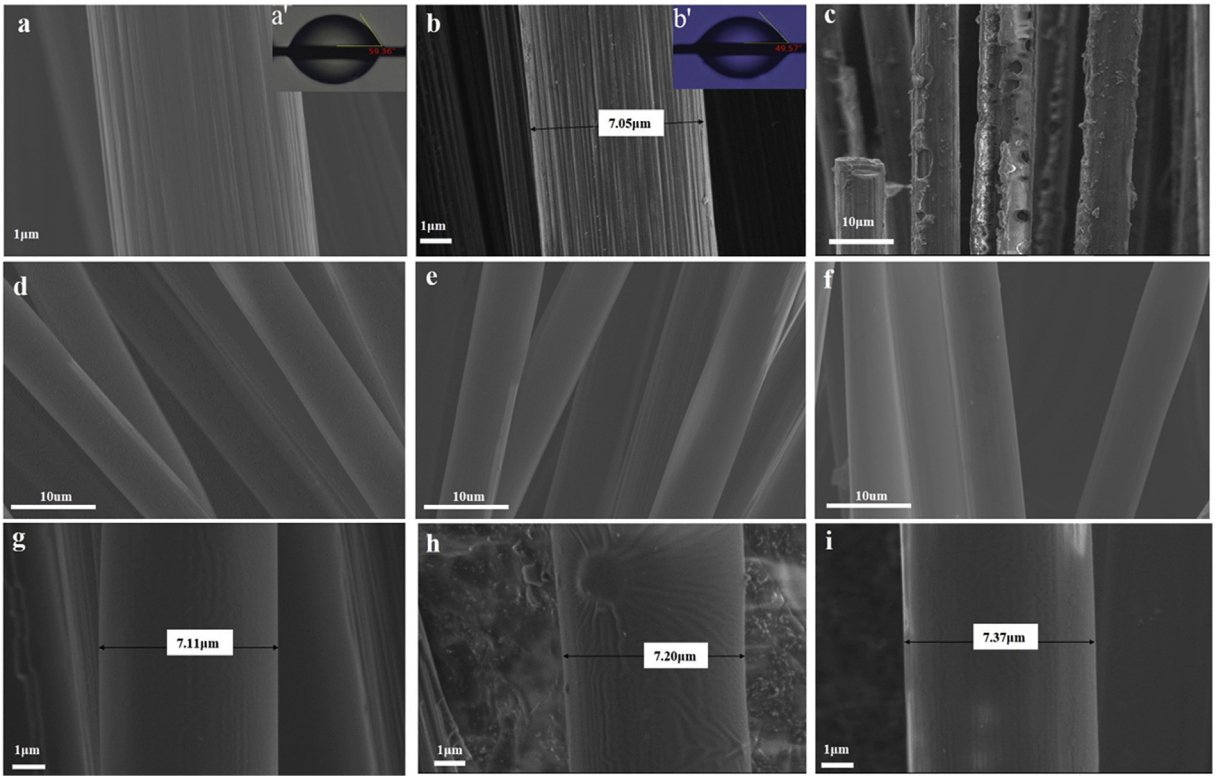

Fig. 3. SEM images of the investigated CFs: (a) CF_{de}; (b) CF_{ox}; (c) CF_{ox}-C; (d) CF_{ox}-Uni-0.06; (e) CF_{ox}-Uni-0.15; (f) CF_{ox}-Uni-0.32; (g)single CF_{ox}-Uni-0.06; (h) single CF_{ox}-Uni-0.15; (i) single CF_{ox}-Uni-0.32.

up to 500 °C. Goud et al. [27] investigated mechanical properties of unidirectional carbon fiber reinforced polypropylene composites in varying forms of fiber, powder and film, in which the composites were made by sandwiching carbon fiber tows between PP films. But in the over-lay process, the overlaid polymers were very hard to impregnated to the carbon fibers, even in high temperature and high pressure, due to the over-long impregnation routine. Comparatively, in this work, a spray-coating and uniformization processes were used so as to obtain uniform coating on the carbon fiber surfaces under relative low temperatures and pressures.

Furthermore, the CF_{ox}-Uni fibers were thoroughly washed with dichloroethane to remove the physically-absorbed resin (denoted as CF_{ox}-Uni-w1), so as to evaluate interactions between the CF_{ox} and the PC coating. The CF_{ox}-Uni fibers were further sandwiched into two PC sheets and moulded for hot-pressing. Thus, the solvent-washed CFs were obtained (CF_{ox}-Uni-w2). As shown in Fig. 4, the PC coating on the CF_{ox}-Uni-w1 was nearly fully washed out; however, some PC residues could still be identified on the CF_{ox}-Uni-w2. This implies that the thermal treatment should afford further interactions between CF_{ox} and its PC coating, in consistent with our previous study [28].

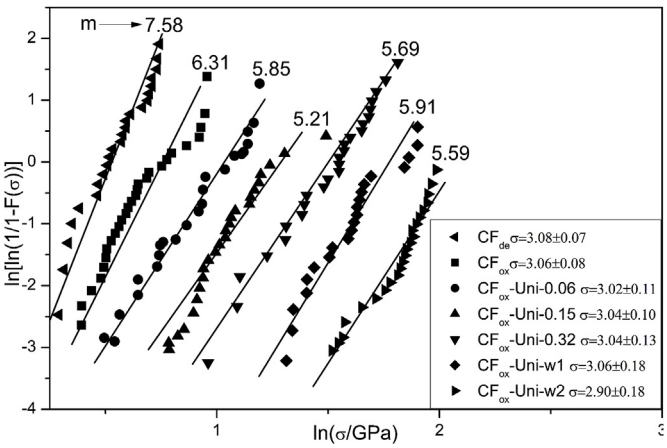

Fig. 5. Weibull modulus data of CF tensile strength.

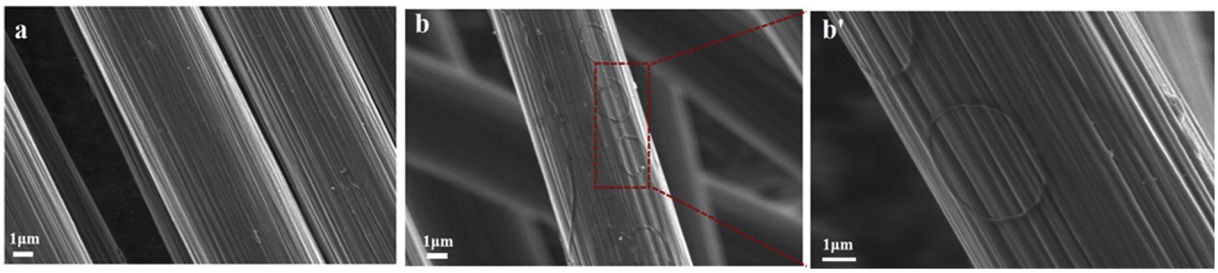

Fig. 4. SEM images of (a) CF_{ox}-Uni-w1; (b) CF_{ox}-Uni-w2 and (b') enlarged image for the selected region in (b).

3.2. Changes in tensile strength of CFs

The tensile strength results of the CFs are plotted in Fig. 5. The CF_{de} exhibited a slightly higher tensile strength value than the CF_{ox}, indicating the oxidation treatment resulted in slightly damages to the CFs. The average tensile strength of the coated CFs decreased slightly compared to that of the untreated CFs (shown in Fig. 5), which could be attributed mainly to the volume effects resulting from the increased fiber diameter [25]. Moreover, compared with CF_{ox}-Uni, the tensile strength of the CF_{ox}-Uni-w2 significantly decreased, resulting from somewhat thermal damages during the imposed hot-pressing.

These tensile strength data were further analyzed by Weibull statistics based on the weakest-linking theory and Weibull modulus (m) determined from the slope of the linearly-fitted straight The Weibull modulus generally indicates scattering extent of the strength data [29]. It can be seen that the Weibull modulus of the treated CFs was smaller than that of the CF_{ox}, indicating that the strength data scattering extent became relatively larger after coating, possibly due to the afterward heating process. Furthermore, the Weibull modulus of the CF_{de} was significantly higher than that of the CF_{ox}, suggesting that the tensile strength scattering extent of CF_{ox} became larger due to the air oxidation.

3.3. Evaluation of CF/PC interfacial properties

The fiber/matrix interfacial properties can be evaluated by observation of stress birefringence patterns at the fiber breaks for the single fiber/PC composites. The birefringence patterns (shown in Fig. 6) became increasingly brighter and concentrated with increasing film thickness, suggesting an improved interfacial adhesion by applying a PC coating. IFSS data (Table 2) showed that thickness of the PC coating on the CFs played an important role in determining the IFSS results for a composite, *i.e.*, with increasing film thickness, the IFSS of the corresponding composites significantly increased. However, from the data in Fig. 7, the further increase in thickness of the PC coating had little effective enhancement on the mechanical properties. In this study, a suitable coating thickness without causing nonhomogeneous coating (as shown in Fig. S3 in the supporting information) was determined to be ranging from 0.15 to 0.32 μm. The interfacial properties are closely related to the goodness of resin impregnation, the better the resin impregnation, the higher the IFSS result [30,31].

The IFSS between CF_{de}-Uni and resin matrix was 27.4 MPa, which exhibited lower value than that of CF_{ox}-Uni/PC when the CFs were spray-coated by a same PC solution concentration (5 wt%). This was due to the oxygenated functionalities on the CF_{ox}. In our previous study, during a hot-pressing process, the oxygenated functionalities, such as C–O, C═O, C(O)O, will generate hydrogen bonding and chemical interaction (such as interesterification interaction) [28]. The similar conclusions were also reported by other researchers. Lee et al. [32] reported that the PC molecular chains could cause polar bonding interactions between carbonyl groups in PC resin and functional groups on the carbon fibers surfaces. Hüttinger et al. [33] correlated the high interlaminar shear strength between CFs and PC to the acid-base interactions during an impregnation process and subsequent chemical reactions during fabricating a composite, resulting from oxygen-containing functional groups on CFs and carbonate groups on the polymers; they also found that the chemical interaction was coupled along with release of carbon dioxide, originating from the decomposition of carboxylic groups. Kamps et al. [34] introduced reactive, functional groups to the PC resin, and by transesterification reactions, forming strong covalent bonding interactions between the modified PC and CFs; they found that the different contents of functional groups will significantly influence the CF/PC interfacial adhesion.

Table 2
The IFSS results for CF/PC unidirectional composites.

	Critical fragmentation length/mm	IFSS/MPa
CF_{ox}	0.88 ± 0.05	19.96 ± 1.75
CF_{ox}-Uni-0.06	0.77 ± 0.05	24.33 ± 2.31
CF_{ox}-Uni-0.15	0.66 ± 0.04	31.91 ± 2.28
CF_{ox}-Uni-0.32	0.56 ± 0.05	37.50 ± 2.45
CF_{de}-Uni	0.75 ± 0.02	27.4 ± 2.15
CF_{ox}-Uni-w1	0.86 ± 0.06	20.86 ± 2.86
CF_{ox}-Uni-w2	0.84 ± 0.07	21.30 ± 2.17

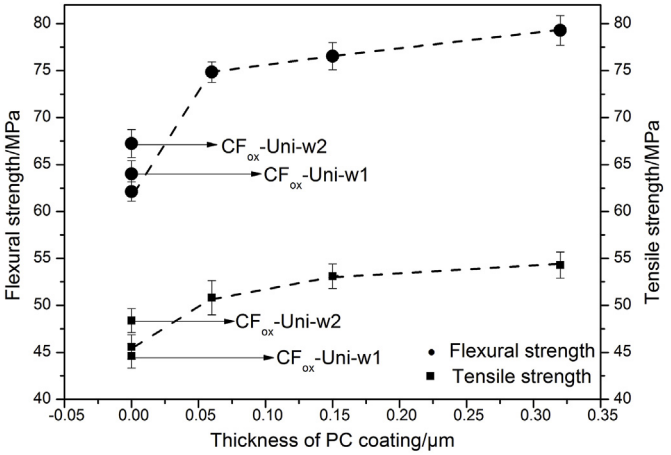

Fig. 7. The relationship between the mechanical strength and thickness of PC coating.

3.4. Evaluation on mechanical properties of the CF/PC composites

The samples were tensile-tested perpendicular to the fiber axis (90° tensile test), and all of them were fractured at the CF/PC interfaces, therefore, the 90° tensile strength could be an indication of the

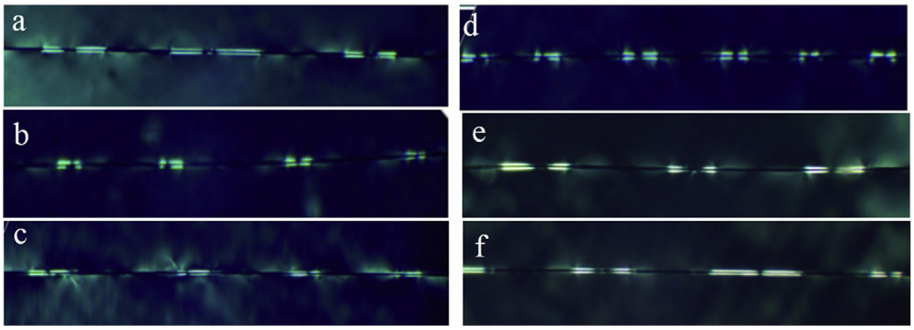

Fig. 6. Birefringence patterns of the CFs composites, in which CFs were coated by PC solution: (a) CF_{ox}; (b) CF_{ox}-Uni-0.06; (c) CF_{ox}-Uni-0.15; (d) CF_{ox}-Uni-0.32; (e) CF_{ox}-Uni-w1; (f) CF_{ox}-Uni-w2.

Table 3
The mechanical properties of the composites.

Sample	Tensile strength/MPa	Flexural strength/MPa
CF_{ox}	45.58 ± 1.30	62.12 ± 1.03
CF_{ox}-Uni-0.06	50.82 ± 1.82	74.84 ± 1.09
CF_{ox}-Uni-0.15	53.10 ± 1.31	75.54 ± 1.45
CF_{ox}-Uni-0.32	54.28 ± 1.40	77.28 ± 1.58
CF_{ox}-Uni-w1	44.62 ± 1.31	64.02 ± 1.39
CF_{ox}-Uni-w2	48.38 ± 1.28	67.23 ± 1.50

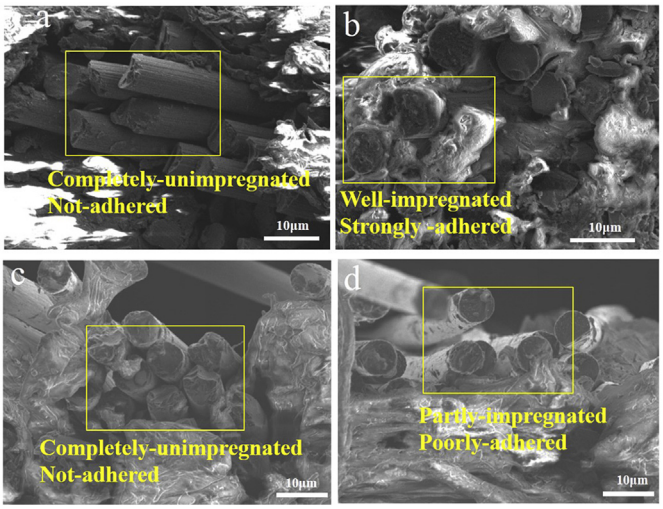

Fig. 8. The 90° tensile-fractographs of the composite laminates: (a) CF_{ox}; (b) CF_{ox}-Uni; (c) CF_{ox}-Uni-w1; (d) CF_{ox}-Uni-w2.

interfacial properties. The mechanical properties of the composites reinforced by the CF_{ox} and various coated CFs are shown in Table 3. With the thickness of the PC coatings increased up to 0.06 μm, both the tensile strength and flexural strength showed a sudden increase, followed by a plateau with a further increase in the thickness (Fig. 7). The tensile strength was improved by a maximum of 19.09% for the CF_{ox}-Uni-0.32 compared with that for the CF_{ox}. The optimal interfacial properties were determined to be the PC thickness of 0.32 μm, which was consistent with the IFSS results. These results implied that mechanical properties of the composites were largely determined by the impregnation of the matrix resin.

The tensile-fractured morphologies of the composite laminates were examined under SEM observation (shown in Fig. 8). The results showed that little resin residues remained on the CF_{ox} and obvious gaps between the CFs and PC resin could be observed, indicating a poor interfacial adhesion. However, when the PC coating was applied onto the CF surfaces, the amount of residual resin adhered to the CF surfaces increased significantly. This observation suggested that the interfacial adhesion between CF_{ox} and PC would become stronger after coating with a PC solution, leading to improved mechanical properties for the composite. Liu [35] et al. prepared Nylon66-reinforced carbon fabric composites by a solution impregnation method, by which the resin was fully impregnated into the fiber bundles, leading to a significantly improved interfacial bonding strength for the CFs/Nylon66 composites. Han [36] et al. also improved the resin impregnation into CF bundles by using polypropylene (PP) solution impregnation, and the interfacial adhesion between a carbon fabric and the PP matrix was promoted.

Moreover, as shown in Fig. 7, the mechanical strength of CF_{ox}-Uni-w2 was significantly higher than that of the CF_{ox}, but the CF_{ox}-Uni-w1 had a low tensile strength data close to the CF_{ox}. The change tendency was consistent with the results of interfacial shear strength (Table 2). The tensile-fractured morphologies of the CF_{ox}-Uni-w1 (Fig. 8c) revealed that the CFs was poorly impregnated by the matrix resin, leading to a very weak adhesion between the CF_{ox}-Uni-w1 and PC resin. However, after the hot-pressing treatment, the adhesion between the CF_{ox}-Uni-w2 and PC could be observed (Fig. 8d), which further confirmed the chemical reactions between the CFs and the PC coating by the heat treatment.

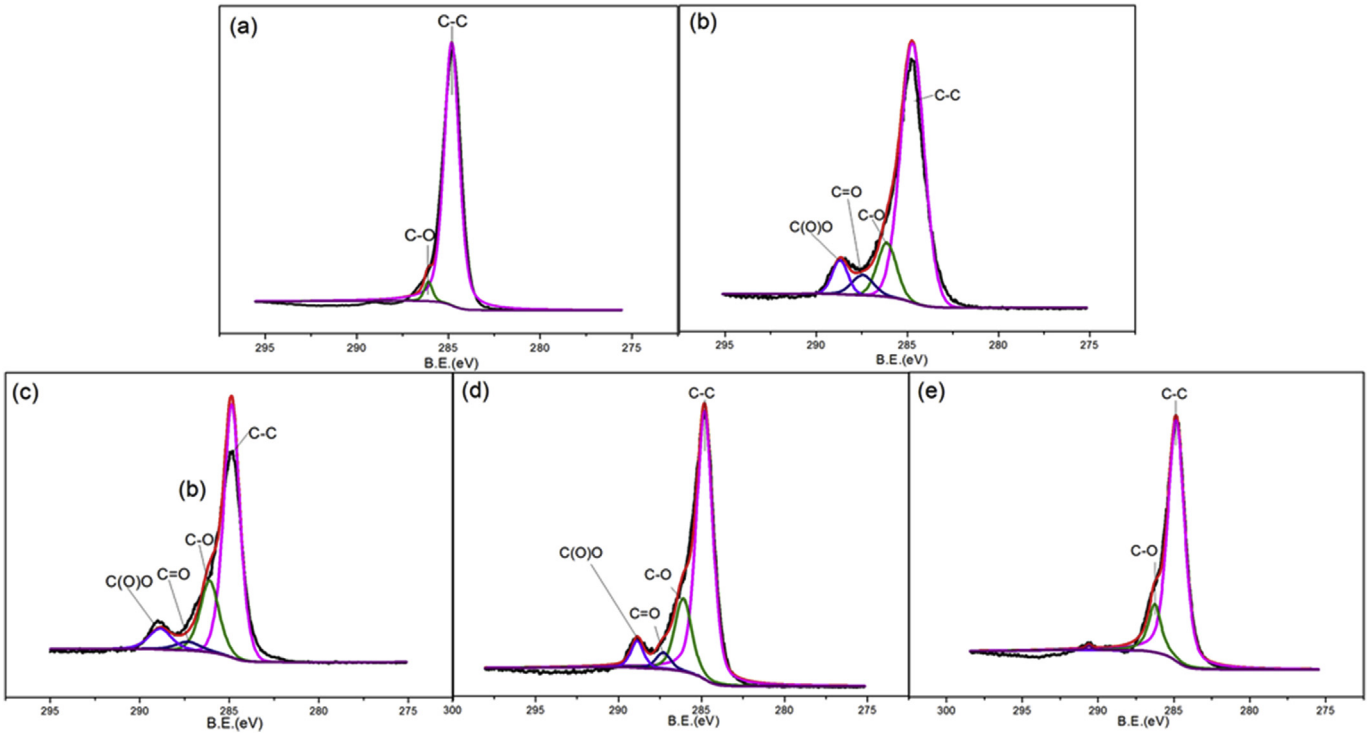

Fig. 9. XPS spectra of the CFs: (a) CF_{de}; (b) CF_{ox}; (c) CF_{ox}-Uni-w1; (d) CF_{ox}-Uni-w2; (e) CF_{de}-Uni-w.

Table 4
Atomic percentage (At%) of carbon functional groups on the CF surfaces.

Binding energy (eV)	CF_{de}	CF_{ox}	CF_{ox}-Uni-w1	CF_{ox}-Uni-w2	CF_{de}-Uni-w
C–C (284.6)	96.22	75.21	73.67	68.45	89.96
C–O (286.1–286.3)	3.78	14.07	15.96	18.95	9.28
C=O (287.3–287.6)	–	2.56	2.58	3.98	–
C(O)O (288.4–288.9)	–	7.77	7.79	8.62	–
Shake up satellites (290.4–290.8)	–	0.38	–	–	0.76

3.5. XPS analyses on interfacial chemistries

The functionalities concentrations of the various CFs were quantitatively determined by XPS analysis. The C1s spectra of these CFs were peak-fitted into five components: C–C, C–O, C═O, C(O)O and Shake up satellites. The results are shown in Fig. 9 and Table 4. For the CF_{ox}-Uni-w1, the contents of C–O, C═O and C(O)O were almost the same as those of the CF_{ox}. But for the CF_{ox}-Uni-w2, the content of oxygen-containing functional groups increased obviously with respect to the non-heated CFs, indicating the hydroxyl or carboxyl groups on the CFs resulting from thermo-reactions during the hot-pressing. To further investigate the impacts of functional groups, a controlled experiment was also done on the CF_{de}-Uni, The CF_{de}-Uni after the hot-pressing and washing treatments was denoted as CF_{de}-Uni-w. The C1s spectrum of CF_{de}-Uni-w (Fig. 9) revealed the presence of only two carbon species belonging to C–C and C–O, but the concentration of C–O was obviously lower than that of CF_{ox}-Uni-w2 (Table 4), indicating that little PC resin was remained on the CF_{de}-Uni-w surfaces. These results suggested that the oxygenated functionalities on CF surfaces would generate chemical bonding with the PC matrix during hot-press treatment. This was in good consistent with the interfacial property results and our previous study [28].

3.6. FTIR analyses on interfacial chemistries

The Fourier transform infrared spectra (Fig. 10a) of the PC resin showed the 1774 cm^{-1} band (carbonyl stretching vibration) and 1226, 1193 and 1162 cm^{-1} bands (stretching vibrations of –C-O-C-), indicating the presence of functional groups in the PC resin. From the FTIR-ATR spectra of the CFs results, it can be concluded that the CF_{ox} and CF_{ox}-Uni-w1 surfaces had stronger peak of –C═C- in a benzene ring (1533/1537 cm^{-1}), however, the spectra (Fig. 10d) of the CF_{ox}-Uni-w2 revealed the presence of C═O (1714 cm^{-1}), –C-O-C-(1068, 1224 cm^{-1}). The absorption peaks at 1714 cm^{-1} were attributed to the C═O symmetric stretching vibration in the ester groups on the fiber surface [37]. The presence of these bands indicated that the PC residue should be chemically-bonded onto the CF_{ox}-Uni-w2, which was formed by the hot-pressing treatment. The differential FTIR spectrum by subjecting the CF_{ox}-Uni-w1 from the CF_{ox}-Uni-w2 can illustrate the generated or consumed chemical species during the heat-treatment. The positive bands 1724 (C═O stretching), 1224 (aromatic C–O-stretching), 1076 (aliphatic C–O stretching) cm^{-1} could be attributed to the generated oxygen functionalities during the hot-pressing. The chemical interactions between CF_{ox} and PC coatings should be favorable for improving the interfacial adhesion.

3.7. Mechanisms on CF/PC interfacial interactions

Based on our study, the CF/PC interfacial adhesion could be related to the resin impregnation and fiber-matrix interactions. The mechanisms were schematically illustrated in Fig. 11. Fig. (a) shows a situation with poor impregnation and weak interfacial interactions, like CF_{ox}/PC or CF_{ox}-Uni-w1/PC. The SEM and XPS results had shown that there existed only physical interaction (*i.e.*, van der Waals forces) between

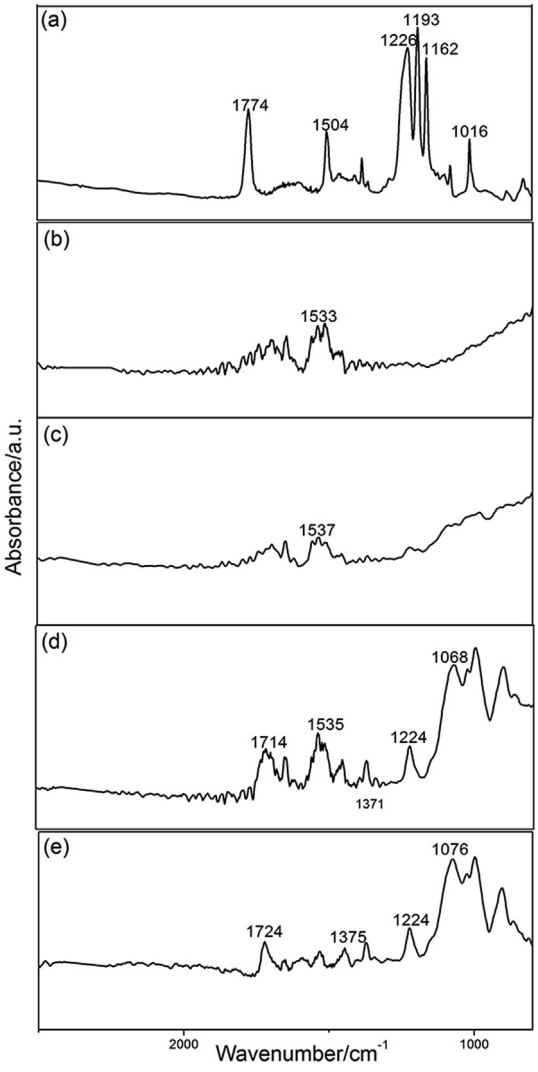

Fig. 10. The FTIR-ATR spectra of the CFs: (a) PC; (b) CF_{ox}; (c) CF_{ox}-Uni-w1; (d) CF_{ox}-Uni-w2; (e) CF_{de}-Uni-w2 - CF_{ox}-Uni-w1 differential.

the CFs and PC coating before hot-pressing. This conclusion was in good agreement with results of the IFSS test (shown in Table 2), which showed almost identical IFSS data for the CF_{ox}-Uni-w1 to that of the CF_{ox}. During hot-pressing, the PC matrix can't easily fully impregnate the carbon fibers tow, which will result in low interfacial shear strength and mechanical properties. Fig. (b) shows a situation with general impregnation and weak interfacial interactions, like CF_{ox}-Uni-w2/PC. The tensile-fractured morphologies of the CF_{ox}-Uni-w2 revealed that the adhesion between the CF_{ox}-Uni-w2 and PC could be observed after the hot-pressing treatment, which confirmed the chemical reactions between the CFs and the PC coating by the heat treatment. However, for the CF_{ox}-Uni-w2, the PC coating was too thin to fully impregnate the CFs during hot-pressing process, which could also result in poor interfacial adhesion. Fig. (c) shows a situation with good impregnation and strong interfacial interactions, like CF_{ox}-Uni/PC. The thermoplastic resin is usually highly viscous at high temperatures, leading to an inadequate impregnation and thus leading to poor-in-resin domains at the final composites. In this study, the PC coating was formed as a pre-impregnated thermoplastic layer with thickness of 0.15–0.32 μm on the CF surfaces, which would be favorable for impregnating the nearby CFs during a thereafter heating process (*e.g.*, hot-press) to improve the interfacial adhesion between the CFs and the thermoplastic matrix, as illustrated in Fig. 11c. Meanwhile, the physical and chemical interaction between functional groups and PC resin also contributed to

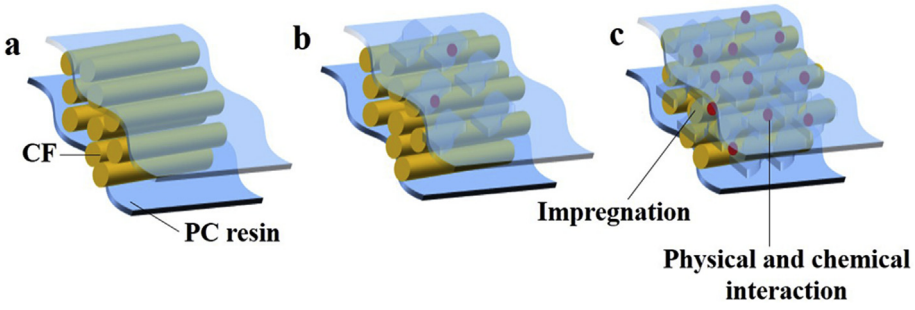

Fig. 11. The mechanism of interphase fracture modes for (a) CF_{ox}; (b) CF_{ox}-Uni-w2; (c) CF_{ox}-Uni.

improved interfacial adhesion. Therefore, the reactions between hydroxyl or carboxyl and carbonate groups and the good impregnation were the reasonable explanation for the enhanced interfacial adhesion.

4. Conclusions

In this study, interfacial adhesion between CFs and PC was enhanced by improving the resin impregnation by using a PC spray-coating on the CFs. The PC coating and a thermal uniformization process had leaded to a well-coated and fully-impregnated thermoplastic layer on the CF surfaces. Meanwhile, the thickness of the PC coating on the CFs played an important role in determining the IFSS results for the corresponding composites; with increasing coating thickness, the IFSS data of the corresponding composites increased initially, and then followed by a plateau. The enhanced interfacial adhesion properties were attributed to not only the good impregnation of the PC resin into the CF bundle, but also to chemical reactions in the interphases induced by a heat treatment, e.g., hot-pressing in this study. Mechanical properties of the composites were also found to be controlled by both interfacial properties of the CF/matrix interfaces and impregnation properties of the matrix resin.

Acknowledgements

This work was supported by Joint Fund of the National Natural Science Foundation of China - Shanxi Province [Grant No. U1810116].

Appendix A. Supplementary data

Supplementary data to this article can be found online at https://doi.org/10.1016/j.compscitech.2019.107763.

References

[1] J.S. Lee, T.J. Kang, Changes in physico-chemical and morphological properties of carbon fiber by surface treatment, Carbon 35 (2) (1997) 209–216 https://doi.org/10.1016/s0008-6223(96)00138-8.
[2] Y.Y. Song, U. Gandhi, T. Sekito, U.K. Vaidya, J. Hsu, A. Yang, T. Osswald, A novel cae method for compression molding simulation of carbon fiber-reinforced thermoplastic composite sheet materials, J. Compos. Sci. 33 (2) (2018) 1–16 https://doi.org/10.3390/jcs2020033.
[3] T.G. Tang, J. Kardos, A review of methods for improving the interfacial adhesion between carbon fiber and polymer matrix, Polym. Compos. 18 (1997) 100–113 https://doi.org/10.1002/pc.10265.
[4] M.A. Montes-Morán, F.W.J. van Hattum, J.P. Nunes, A. Martínez-Alonso, J.M.D. Tascón, C.A. Bernardo, A study of the effect of plasma treatment on the interfacial properties of carbon fibre–thermoplastic composites, Carbon 43 (8) (2005) 1795–1799 https://doi.org/10.1016/j.carbon.2005.02.005.
[5] V.K. Raghavendran, L.T. Drzal, P. Askeland, Effect of surface oxygen content and roughness on interfacial adhesion in carbon fiber-polycarbonate composites, J. Adhes. Sci. Technol. 16 (10) (2002) 1283–1306 https://doi.org/10.1163/156856102320252813.
[6] C. Ozkan, N. Gamze Karsli, A. Aytac, V. Deniz, Short carbon fiber reinforced polycarbonate composites: effects of different sizing materials, Compos. B: Eng. Times 62 (2014) 230–235 https://doi.org/10.1016/j.compositesb.2014.03.002.
[7] S.A. Song, C.K. Lee, Y.H. Bang, S.S. Kim, A novel coating method using zinc oxide nanorods to improve the interfacial shear strength between carbon fiber and a thermoplastic matrix, Compos. Sci. Technol. 134 (2016) 106–114 https://doi.org/10.1016/j.compscitech.2016.08.012.
[8] F. Vautard, P. Fioux, L. Vidal, F. Siffer, V. Roucoules, J. Schultz, M. Nardin, B. Defoort, Use of plasma polymerization to improve adhesion strength in carbon fiber composites cured by electron beam, ACS Appl. Mater. Interfaces 6 (3) (2014) 1662–1674 https://doi.org/10.1021/am4045663.
[9] V.K. Raghavendran, L.T. Drzal, Fiber-matrix interfacial adhesion improvement in carbon fiber-bisphenol-a polycarbonate composites by polymer grafting, J. Adhes. 78 (10) (2010) 895–922 https://doi.org/10.1080/00218460290010476.
[10] Q.Y. Peng, X.D. He, Y.B. Li, C. Wang, R.G. Wang, P.A. Hu, Chemically and uniformly grafting carbon nanotubes onto carbon fibers by poly(amidoamine) for enhancing interfacial strength in carbon fiber composites, J. Mater. Chem. 22 (2012) 5928–5931 https://doi.org/10.1039/c2jm16723a.
[11] S.Y. Huang, G.P. Wu, C.M. Chen, Y. Yang, S.C. Zhang, C.X. Lu, Electrophoretic deposition and thermal annealing of a graphene oxide thin film on carbon fiber surfaces, Carbon 52 (2013) 613–616 https://doi.org/10.1016/j.carbon.2012.09.062.
[12] J.O. Iroh, K.M.S. Jordan, Mechanical properties of carbon fibre/PMR-15 composites containing thermoplastic polyimide interphase coatings, Sur. Eng. 16 (4) (2013) 303–308 https://doi.org/10.1179/026708400101517288.
[13] M.A. Montes-Morán, A. Martínez-Alonso, J.M.D. Tascón, M.C. Paiva, C.A. Bernardo, Effects of plasma oxidation on the surface and interfacial properties of carbon fibres/polycarbonate composites, Carbon 39 (2001) 1057–1068 https://doi.org/10.1016/S0008-6223(00)00220-7.
[14] T. Yamamoto, K. Uematsu, T. Irisawa, Y. Tanabe, Controlling of the interfacial shear strength between thermoplastic resin and carbon fiber by adsorbing polymer particles on carbon fiber using electrophoresis, Compos. A: Appl. Sci. Manufacturing 88 (2016) 75–78 https://doi.org/10.1016/j.compositesa.2016.05.021.
[15] F.R. Jones, A review of interphase formation and design in fibre-reinforced composites, J. Adhes. Sci. Technol. 24 (1) (2010) 171–202 https://doi.org/10.1163/016942409X12579497420609.
[16] I.Y. Chang, J.K. Lees, Recent development in thermoplastic composites a review of matrix systems and processing methods, J. Thermoplast. Compos. Mater. 1 (1988) 277–295 https://doi.org/10.1177/089270578800100305.
[17] M. Guigon, E. Klinklin, The interface and interphase in carbon fiber-reinforced composites, Composites 25 (7) (1994) 534–539 https://doi.org/10.1016/0010-4361(94)90181-3.
[18] R.R. Chary, D.E. Hirt, Coating carbon fibers with a thermoplastic polyimide using aqueous foam, Polym. Compos. 15 (4) (1994) 306–311 https://doi.org/10.1002/pc.750150409.
[19] G.M. Wu, J.M. Schultz, G.M. Wu, Processing and properties of solution impregnated carbon fiber reinforced polyether sulfone composites, Polym. Compos. 21 (2) (2000) 223–230 https://doi.org/10.1002/pc.10179.
[20] C. Steggall-Murphy, P. Simacek, S.G. Advani, S. Yarlagadda, S. Walsh, A model for thermoplastic melt impregnation of fiber bundles during consolidation of powder-impregnated continuous fiber composites, Compos. A: Appl. Sci. Manufacturing 41 (1) (2010) 93–100 https://doi.org/10.1016/j.compositesa.2009.09.026.
[21] J.W. Kim, J.S. Lee, The effect of the melt viscosity and impregnation of a film on the mechanical properties of thermoplastic composites, Materials 9 (6) (2016) 1–15 https://doi.org/10.3390/ma9060448.
[22] H.F. Wu, Weibull analysis of strength-length relationships in single Nicalon SiC fibres, J. Mater. Sci. 27 (1992) 3318–3324 https://doi.org/10.1007/BF01116031.
[23] E.M. Asloun, J.B. Donnet, G. Guilpain, M. Nardin, J. Schultz, On the estimation of the tensile strength of carbon fibres at short lengths, J. Mater. Sci. 24 (1989) 3504–3510 https://doi.org/10.1007/bf02385732.
[24] A. Kelly, W.R. Tyson, Tensile properties of fiber-reinforced metals: copper/tuxstes and copper/molybdenum, J. Mech. Phys. Solids 13 (1965) 329–350 https://doi.org/10.1016/0022-5096(65)90035-9.
[25] K.L. Pickering, T.L. Murray, Weak link scaling analysis of high-strength carbon fibre, Compos. A 30 (1999) 1017–1021 https://doi.org/10.1016/S1359-835X(99)00003-2.
[26] H.M. EL-Dessouky, C.A. Lawrence, Ultra-lightweight carbon fibre/thermoplastic composite material using spread tow technology, Compos. B 50 (2013) 91–97 https://doi.org/10.1016/j.compositesb.2013.01.026.
[27] V. Goud, R. Alagirusamy, A. Dasa, D. Kalyanasundaram, Influence of various forms of polypropylene matrix (fiber, powder and film states) on the flexural strength of carbon-polypropylene composites, Compos. B 166 (2019) 56–64 https://doi.org/10.1016/j.compositesb.2018.11.135.

[28] T.T. Yao, G.P. Wu, C. Song, Interfacial adhesion properties of carbon fiber/polycarbonate composites by using a single-filament fragmentation test, Compos. Sci. Technol. 149 (2017) 108–115 https://doi.org/10.1016/j.compscitech.2017.06.017.

[29] S.R. Dai, M.R. Piggott, The strengths of carbon and kevlar fibres as a function of their lengths, Compos. Sci. Technol. 49 (1) (1993) 81–87 https://doi.org/10.1016/0266-3538(93)90024-B.

[30] M.Y. Jia, C.X. Li, P. Xue, K. Chen, T.H. Chen, Research on the melt impregnation of continuous carbon fiber reinforced nylon 66 composites, IOP Conf. Ser. Mater. Sci. Eng. 137 (2016) 012–053 https://doi.org/10.1088/1757-899X/137/1/012053.

[31] S. Kobayashi, T. Tsukada, T. Morimoto, Resin impregnation behavior in carbon fiber reinforced polyamide 6 composite: effects of yarn thickness, fabric lamination and sizing agent, Compos. A: Appl. Sci. Manufacturing 101 (2017) 283–289 https://doi.org/10.1016/j.compositesa.2017.06.030.

[32] J.Y. Lee, L.T. Drzal, Surface characterization and adhesion of carbon fibers to epoxy and polycarbonate, Int. J. Adhesion Adhes. 25 (2005) 389–394 https://doi.org/10.1016/j.ijadhadh.2004.11.003.

[33] K.J. Hüttinger, C. Krekel, U. Zielke, Evidence for chemical bond formation between surface treated carbon fibres and high temperature thermoplastics, J. Appl. Polym. Sci. 51 (1991) 737–742 https://doi.org/10.1002/app.1994.070510420.

[34] J.H. Kamps, C. Scheffler, F. Simon, R. Heijden, N. Verghese, Functional polycarbonates for improved adhesion to carbon fibre, Compos. Sci. Technol. 167 (2018) 448–455 https://doi.org/10.1016/j.compscitech.2018.08.035.

[35] B. Liu, A. Xu, L. Bao, Preparation of carbon fiber-reinforced thermoplastics with high fiber volume fraction and high heat-resistant properties, J. Thermoplast. Compos. Mater. 30 (5) (2015) 724–737 https://doi.org/10.1177/0892705715610408.

[36] S.H. Han, H.J. Oh, S.S. Kim, Evaluation of the impregnation characteristics of carbon fiber-reinforced composites using dissolved polypropylene, Compos. Sci. Technol. 91 (2014) 55–62 https://doi.org/10.1016/j.compscitech.2013.11.021.

[37] H.J. Yuan, S.C. Zhang, C.X. Lu, S.Q. He, F. An, Improved interfacial adhesion in carbon fiber/polyether sulfone composites through an organic solvent-free polyamic acid sizing, Appl. Surf. Sci. 279 (2013) 279–284 https://doi.org/10.1016/j.apsusc.2013.04.085.